JOM, Vol. 69, No. 12, 2017
DOI: 10.1007/s11837-017-2598-x

Surface Morphology and Corrosion Behavior of Hydroxyapatite-Coated Co-Cr Implant: Effect of Sintering Conditions

MOSTAFA REZAZADEH SHIRDAR[1,2]
and MOHAMMAD MAHDI TAHERI[1,2,3]

1.—Department of Bioengineering, University of Illinois at Chicago, 851 S. Morgan St, Chicago, IL 60607, USA. 2.—Institute of Biomaterials, Tribocorrosion and Nanomedicine (IBTN), 851 S. Morgan St, Chicago, IL 60607, USA. 3.—e-mail: taheri@uic.edu

The surface morphology and corrosion behavior of a hydroxyapatite (HA)-coated cobalt-chromium (Co-Cr) implant after sintering posttreatment using different times and temperatures were investigated. The substrates were electrophoretically coated with calcium phosphate in solution of $Ca(NO_3)\cdot 4H_2O$ and $NH_4H_2PO_4$. Sintering at four different conditions was then performed on the as-deposited samples. Scanning electron microscopy, contact angle measurement, and potentiodynamic polarization studies were employed to investigate the surface morphology, porosity, wettability, and corrosion behavior of the coated samples. The results revealed that the HA-coated substrate sintered at temperature of 600°C for 20 min showed fairly uniform microstructure with the highest density and corrosion resistance compared with the other conditions. Moreover, the highest wettability was exhibited by the HA surface sintered at temperature of 500°C for 60 min.

INTRODUCTION

Cobalt chromium (Co-Cr) alloy is widely used as metallic biomaterial in many orthopedic applications owing to its high biocompatibility and excellent mechanical properties such as high stiffness as well as wear resistance.[1,2] However, its poor level of osseointegration and high release of toxic ions such as Co and Cr into human body fluids remain matters of concern.[3] Therefore, improving the bioactivity of the surface of Co-Cr and reducing its corrosion are essential for clinical applications of implants using this material.[4]

Due to the good biocompatibility as well as bioactivity of hydroxyapatite (HA), it has great potential for use in orthopedic and dental applications.[5,6] It has been reported that deposition of a HA layer on implants made from metallic materials such as Co-Cr results in improved surface bioactivity and reduced ion release.[7] The similarity of hydroxyapatite [$Ca_{10}(PO_4)_6(OH)_2$] to the main inorganic component of hard tissues (bone) in the human body makes it a suitable replacement material for use in orthopedic applications.[8,9] Owing to the structure and chemical composition of HA, it can promote bone cell growth and bone resorption activity, resulting in formation of chemical bonding (osseointegration) between the implant and tissue.[10] However, the poor mechanical properties of HA coating layers make them unsuitable for use in many load-bearing applications.[11,12]

Sintering posttreatment is considered to be one of the promising surface modification techniques for improving the mechanical properties of HA coating layers.[7] It has been reported that sintering posttreatment can affect the biocompatibility, corrosion resistance, and adhesion strength of such coated implants.[13,14] Although sintering posttreatment is considered to be an excellent surface modification method for enhancing the mechanical properties of HA coating layers,[7] high sintering temperature leads to degradation of HA and the metal substrate while low sintering temperature results in a HA coating layer with high porosity and weak bonding.[15] It has been reported that high sintering temperature may induce crack formation on the surface of the HA coating layer owing to thermal expansion coefficient mismatch.[16] In addition, the

(Published online October 5, 2017)

sintering time strongly influences the amount of crystalline apatite phase present.[17,18] Therefore, the sintering posttreatment parameters of time and temperature are considered to be two critical factors determining the quality and performance of HA coated layers, potentially affecting their coating properties.[14]

The cellular response to an implant is strongly influenced by its microtopography or surface texture.[19] For instance, hydrophilicity or high wettability of the implant surface enhances clinical success rates of implantation. It has been reported that increasing the surface wettability of the implant surface accelerates osseointegration and bone formation by enhancing osteoblast maturation in vitro.[2,20] Rausch-fan et al.[21] and Zhao et al.[22] reported that the hydrophilic nature of the implant surface strongly influences growth factor production and cell differentiation. The importance of porosity and pore structure for osteogenesis has also been extensively investigated.[23] It has been reported that porous structure of HA coatings is essential for implant fixation via bone ingrowth into the pores.[24]

Among several possible techniques for HA coating, including plasma spraying, sol–gel technique, electrophoretic deposition (EPD), pulsed laser deposition, biomimetic coating, and investment casting, the EPD technique has attracted considerable attention due to its simple setup, ability to deposit on complex shapes with different dimensions, low temperature, high efficiency, and short processing time.[7,25] In this study, HA was deposited on Co-Cr substrates using the EPD technique. Sintering posttreatment using four different conditions was then performed on coated samples to investigate the morphology and corrosion behavior of the coated substrates.

MATERIALS AND METHODS

A rod of high-carbon Co-28Cr-6Mo (ASTM F1537) with diameter of 10 mm was cut into disks with thickness of 2 mm. Samples were polished using abrasive silicon carbide papers, then cleaned ultrasonically using acetone. Electrolyte consisting of $Ca(NO_3)_2{\cdot}4H_2O$ and $NH_4H_2PO_4$ in deionized (DI) water with pH of 5 and Ca/P ratio of 1.67 was prepared. The prepared electrolyte was then stirred at 400 rpm for 12 h. The EPD process was conducted using a regulated direct-current (DC) power supply (DYY-6C, BEIJING LIUYI) at current density of 12 mA cm^{-2}. The deposition process was carried out for 20 min at temperature of 25°C using a graphite electrode as anode with the substrate acting as cathode. Subsequently, the coated samples were removed from the electrolyte and rinsed in distilled water. The samples were then oven dried at 60°C for 24 h before conducting sintering posttreatment. Finally, the prepared samples were sintered in a muffle furnace with setpoint ramp rate (SP.rr) of 10°C min^{-1} under four different conditions, viz. 500°C for 20 min, 500°C for 60 min, 600°C for 20 min, and 600°C for 60 min. The corrosion behavior of the coated samples was investigated using potentiodynamic polarization studies according to ASTM standard G5. The tests were carried out in 500 mL Kokubo simulated body fluid (SBF) using a potentiostat corrosion test machine (Princeton Applied Research, AMETEK, versaSTAT 3) with a three-electrode cell. The surface wettability of HA-coated samples was measured using contact angle measurements based on a water droplet (VCA optima, AST) as stated in ASTM standard D7334-08. A droplet of water (1 ± 0.1 μL) was dropped onto the surface of the coated layer, and the contact angle measured at a specified time (5 s).

RESULTS AND DISCUSSION

The surface morphology of HA-coated Co-Cr substrates before and after sintering posttreatment is shown in Fig. 1. The top-view scanning electron microscopy (SEM) image of the coated substrate before sintering is illustrated in Fig. 1a. HA clearly formed on the surface of the Co-Cr alloy without any visible cracking, confirming the eligibility of the coated layer for the subsequent sintering process. The morphology of the HA-coated substrate after sintering at 500°C for 20 min is presented in Fig. 1b, revealing an uncracked coating layer with nonuniform microstructure. It can be interpreted that, when applying this sintering condition, some areas of the coating layer remained unchanged. A SEM image of the HA coating layer after sintering posttreatment at 500°C for 60 min is illustrated in Fig. 1c. The uncracked surface morphology shows more regular structure compared with after sintering at 500°C for 20 min in Fig. 1b. It is noteworthy that, on increasing the sintering time from 20 to 60 min, only a few parts remained unchanged. Figure 1d shows the surface morphology of the HA coated layer after sintering posttreatment at 600°C for 20 min, illustrating a dramatic change in the morphology of the coating surface after sintering under this condition. This fairly uniform coating layer may indicate that most of the amorphous phase was transformed to crystalline HA after sintering posttreatment at this condition.[14] Such an uncracked and homogeneous layer of crystalline HA may improve the mechanical and electrochemical properties of the coated sample.[4] A SEM image of a HA-coated layer after sintering posttreatment at 600°C for 60 min is presented in Fig. 1e. It can be observed that, on increasing the sintering time from 20 to 60 min, some flakes merged together to form an irregular structure, possibly including apatite, tricalcium phosphate (TCP), and calcium oxide (CaO).[26] Therefore, the grains did not have well-defined shape and formed with different sizes. Creation of different calcium phosphate phases after sintering under these four conditions was reported in our previous study.[14]

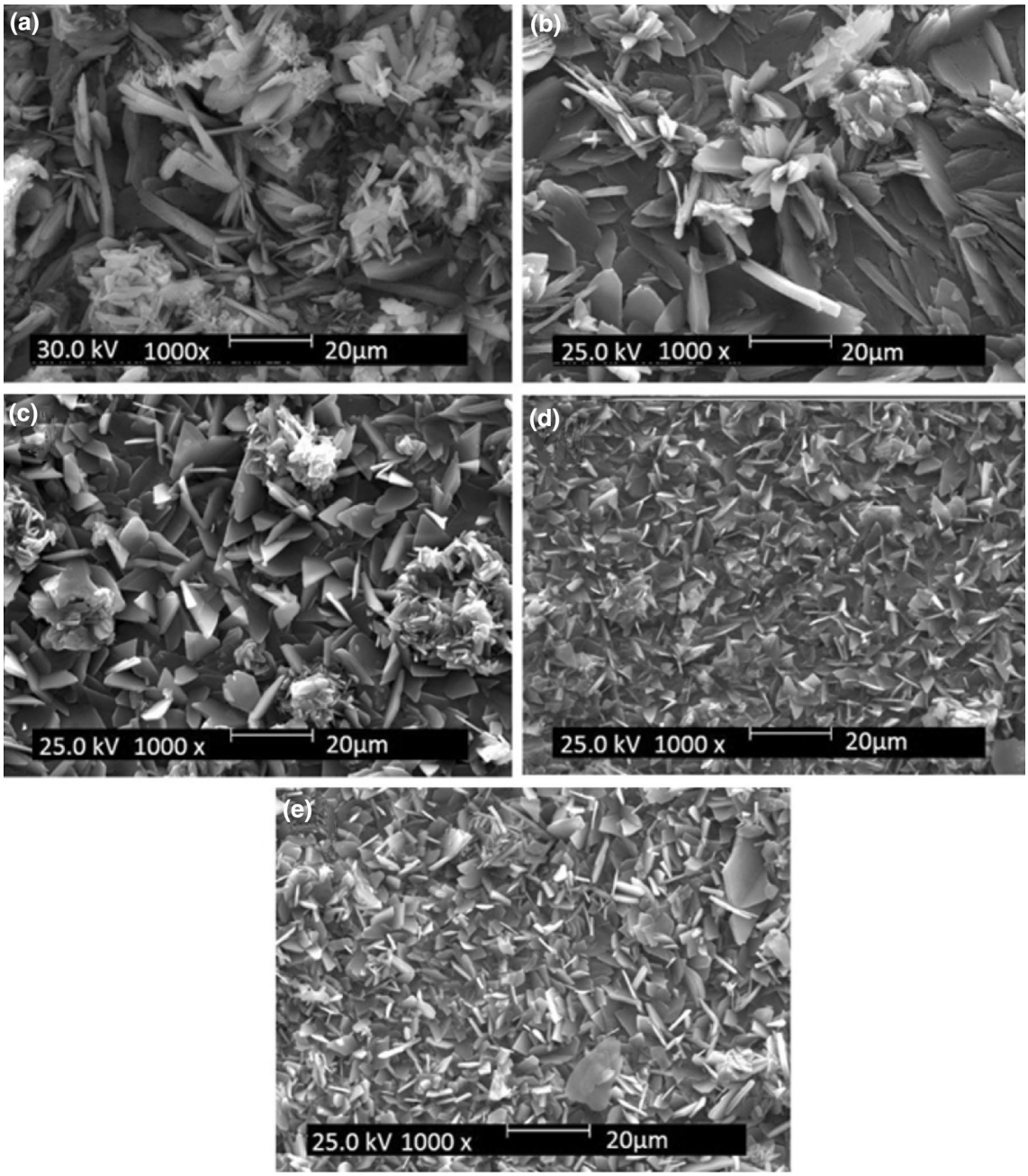

Fig. 1. SEM images of HA-coated Co-Cr: (a) before sintering and after sintering at (b) 500°C for 20 min, (c) 500°C for 60 min, (d) 600°C for 20 min, (e) 600°C for 60 min.

Figure 2 presents the surface porosity of HA-coated substrates sintered under different conditions. Applying a threshold to separate the two classes (with red color in the image indicating porous area) allows measurement of the porosity area percentage, revealing values of 39%, 31%, 23%, and 27% for the samples sintered at 500°C for 20 min, 500°C for 60 min, 600°C for 20 min, and 600°C for 60 min, respectively. This implies that sintering of the HA-coated layer at 600°C for 20 min resulted in the minimum porosity and densest microstructure compared with the other sintering conditions. HA with such dense structure may exhibit enhanced mechanical as well as electrochemical properties.[27]

Potentiodynamic polarization curves of noncoated and HA-coated Co-Cr sintered under different conditions are shown in Fig. 3. The corrosion potential (E_{corr}) and corrosion current density (I_{corr}) of the substrates were obtained from the point at which the slope lines of the curves meet each other.[14] The corresponding values of E_{corr}, I_{corr}, and the corrosion

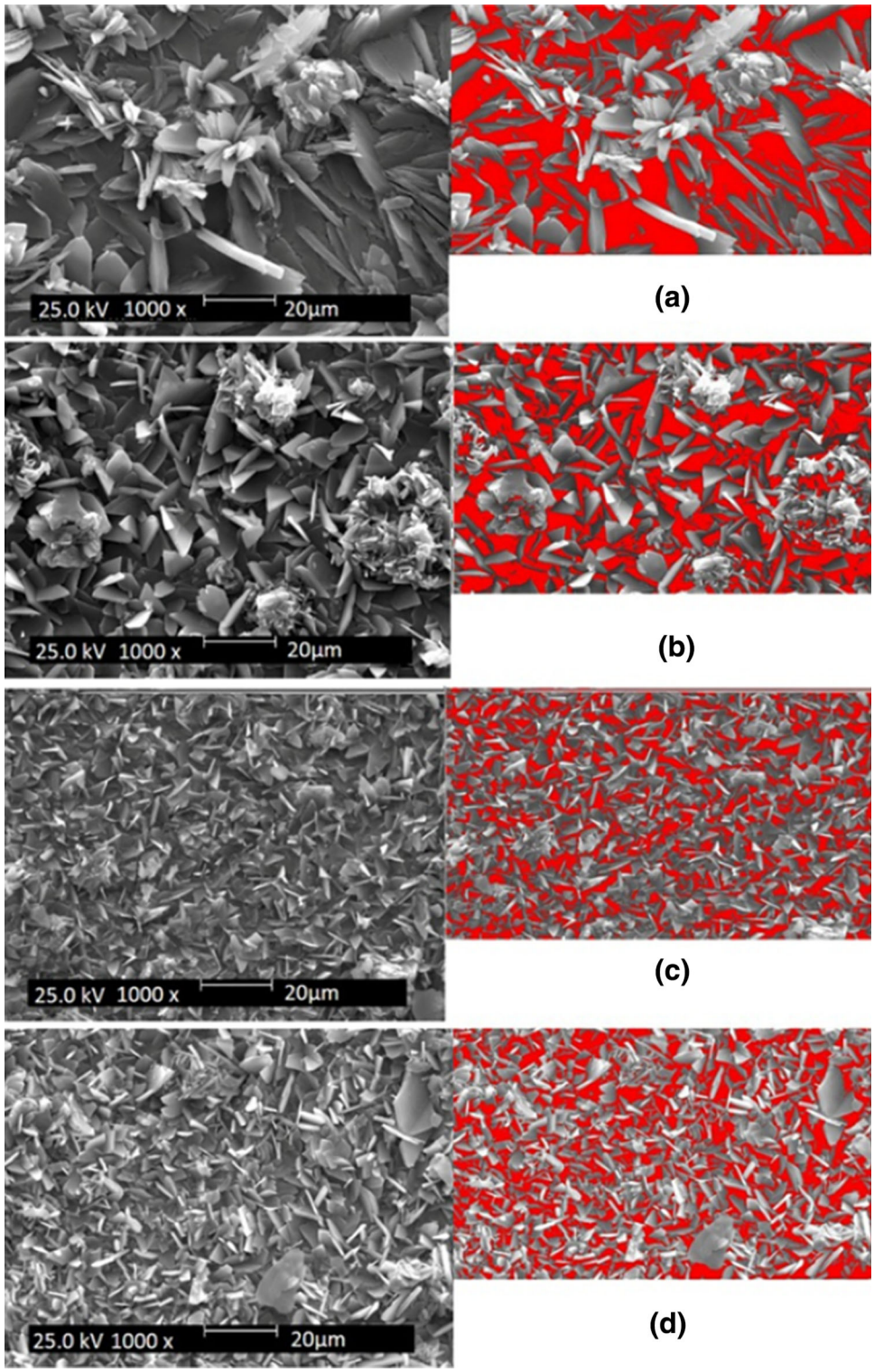

Fig. 2. Image analysis showing porosity of HA coating layers after sintering at (a) 500°C for 20 min, (b) 500°C for 60 min, (c) 600°C for 20 min, (d) 600°C for 60 min.

rate for the noncoated sample were – 625 mV, 3.69 μA and 0.0412 mmPY, respectively, as shown in Fig. 3a. Generally, the corrosion current is directly related to the corrosion rate.[28] Therefore, lower corrosion current results in lower corrosion rate, and vice versa. The potential versus current plot for the coated substrate sintered at 500°C for 20 min is presented in Fig. 3b. The electrochemical results

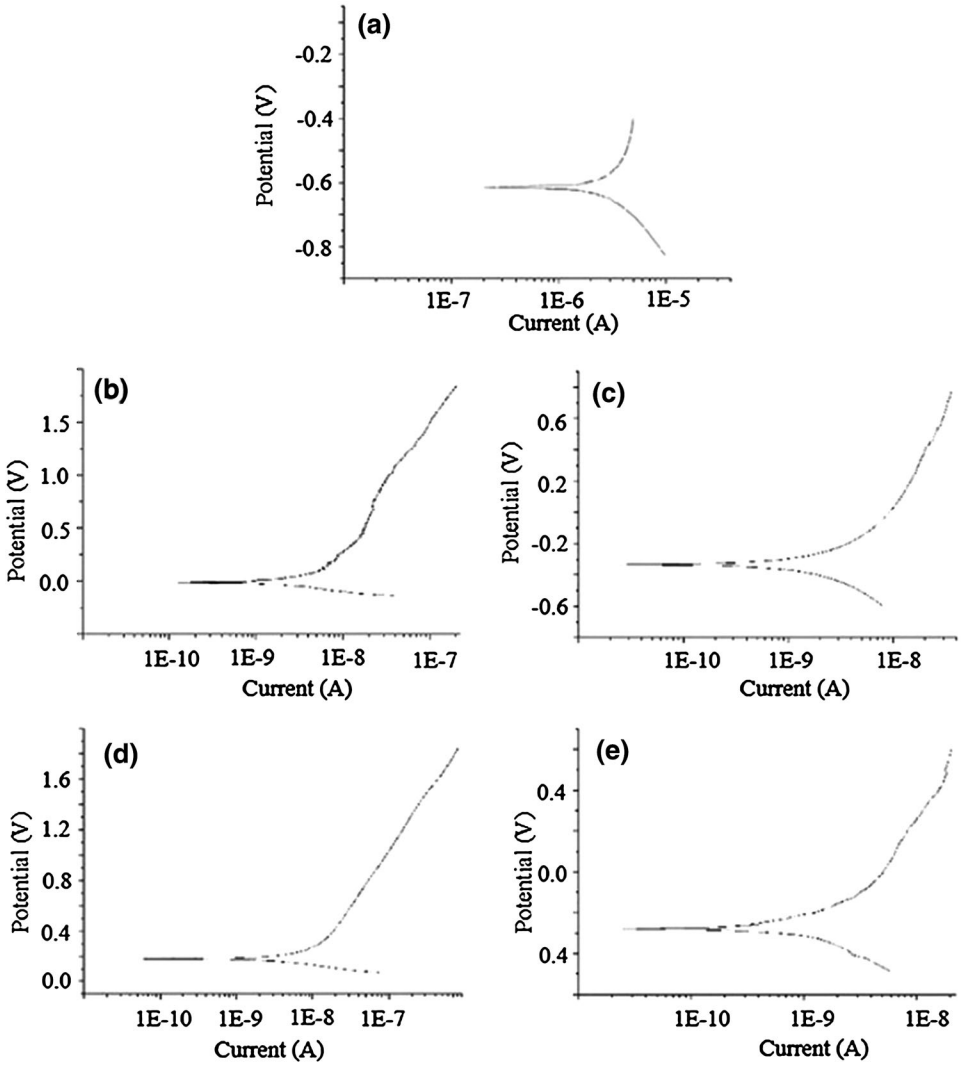

Fig. 3. Potentiodynamic polarization curves of (a) noncoated Co-Cr and HA-coated Co-Cr sintered at (b) 500°C for 20 min, (c) 500°C for 60 min, (d) 600°C for 20 min, (e) 600°C for 60 min.

indicated that the I_{corr}, E_{corr}, and corrosion rate values for this HA-coated sample were 2.158 nA, − 11.859 mV, and 5.7448×10^{-5} mmPY, respectively. Due to the insulating nature[29] and high thermodynamic stability[30] of the HA structure, HA coating decreased the corrosion rate of the Co-Cr alloy. The potentiodynamic polarization curve of the HA-coated sample sintered at 500°C for 60 min is presented in Fig. 3c, indicating I_{corr}, E_{corr}, and corrosion rate values of 747.147 pA, − 333.348 mV, and 1.9881×10^{-5} mmPY, respectively, for this sample. In comparison with the HA-coated sample sintered at 500°C for 20 min, this reduction in corrosion rate can be explained based on the higher density of this coating layer and its possibly greater transformation of amorphous to crystalline phase.[14] This lower corrosion rate indicates lower release of Co and Cr ions from the substrate to the SBF.[31] Figure 3d shows the corrosion curve of the HA-coated Co-Cr implant after sintering posttreatment at 600°C for 20 min, revealing I_{corr}, E_{corr}, and corrosion rate values of 9.849 nA, 178.321 mV, and 0.00026209 mmPY, respectively, for this sample. This improvement in corrosion resistance is related to the low porosity of this HA coating layer, which may provide fewer channels for Co or Cr ions to pass through the coating layer to reach the SBF.[32] This means that, after sintering under this condition, the porosity of the coating layer was reduced, possibly owing to the excessive growth of the HA grains, which filled the empty spaces between grains.[14,32] The I_{corr}, E_{corr}, and corrosion rate values for this HA coated sample sintered at 600°C for 60 min were 407.676 pA, − 278.473 mV, and 1.0848×10^{-5} mmPY, respectively, as shown in Fig. 3e. Compared with the sample sintered at 600°C for 20 min, the corrosion rate of this sample was decreased. This may be

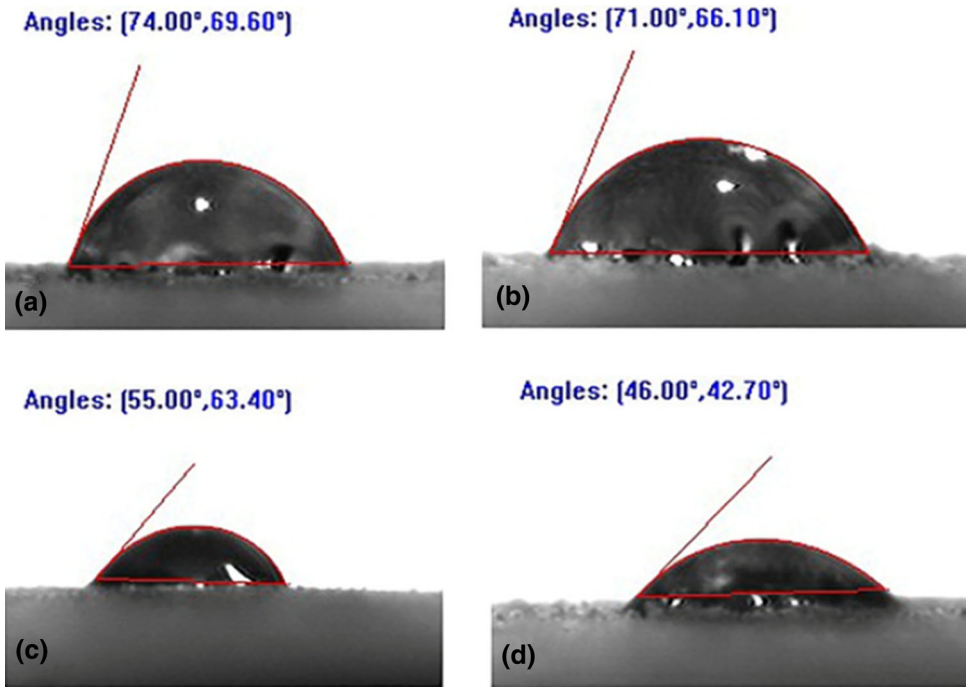

Fig. 4. Contact angle of water droplets measured on of HA coated layers sintered at (a) 500°C for 20 min, (b) 500°C for 60 min, (c) 600°C for 20 min, (d) 600°C for 60 min.

related to the formation of different phases (HA crystalline, TCP, and CaO)[14] and the creation of some nanocracks due to the growth of flakes under this sintering condition.

The hydrophilic nature of the HA-coated samples sintered under different conditions was evaluated by wettability test. The contact angle results for the HA-coated samples are shown in Fig. 4, revealing values of 74°, 71°, 55°, and 46° for the coated samples sintered at 500°C for 20 min, 500°C for 60 min, 600°C for 20 min, and 600°C for 60 min, respectively. It is considered that higher degree of surface hydrophilicity is more desirable for medical implants[33,34] because it can promote new bone formation.[35,36] Based on these findings, the HA-coated sample sintered at 500°C for 20 min exhibited the lowest hydrophilicity while the HA-coated sample sintered at 600°C for 60 min showed the highest degree of hydrophilicity. This may be related to the surface characteristics, such as surface topography, and the chemistry of the HA coated layer. Therefore, it seems that the sintering condition of 600°C for 60 min results in a coating layer with a texture which is more suitable for implant applications.

CONCLUSION

HA was coated on Co-Cr alloy by EPD technique. The coated samples were then sintered using different times and temperatures. The findings reveal that the sintering condition played a remarkable role in the surface morphology and corrosion behavior of the HA-coated substrates. SEM images of coated samples revealed that sintering posttreatment at 600°C for 20 min resulted in a fairly uniform microstructure with the lowest porosity. In addition, potentiodynamic polarization measurements indicated that the HA-coated sample sintered under this condition exhibited the lowest corrosion rate compared with the other conditions. Wettability testing of coated samples after sintering at different conditions indicated that the samples sintered at 600°C for 60 min and 500°C for 60 min possessed the highest and lowest hydrophilicity, respectively.

REFERENCES

1. M.R. Shirdar, S. Izman, M.M. Taheri, M. Assadian, and M.R. Abdul Kadir, *Arab. J. Sci. Eng.* 41, 591 (2016).
2. M.R. Shirdar, S. Izman, M.M. Taheri, M. Assadian, and M.R.A. Kadir, *Arab. J. Sci. Eng.* 40, 1197 (2015).
3. M. Bahrami, M.H. Fathi, and M. Ahmadian, *Mater. Sci. Eng. C Mater. Biol. Appl.* 48, 572 (2015).
4. M.R. Shirdar, M.M. Taheri, H. Moradifard, A. Keyvanfar, A. Shafaghat, T. Shokuhfar, and S. Izman, *Ceram. Int.* 42, 6942 (2016).
5. M.M. Taheri, M.R.A. Kadir, T. Shokuhfar, A. Hamlekhan, M. Assadian, M.R. Shirdar, and A. Mirjalili, *Ceram. Int.* 41, 9867 (2015).
6. W. Chen, B. Tian, Y. Lei, Q.F. Ke, Z.A. Zhu, and Y.P. Guo, *Mater. Sci. Eng., C* 67, 395 (2016).
7. M. Assadian, M. Rezazadeh Shirdar, M.H. Idris, S. Izman, D. Almasi, M.M. Taheri, and M. Abdul Kadir, *Arab. J. Sci. Eng.* 40, 923 (2015).
8. M.M. Taheri, M. Rezazadeh Shirdar, A. Keyvanfar, and A. Shafaghat, *J. Exp. Nanosci.* 12, 83 (2016).
9. M.R. Shirdar, M.M. Taheri, S. Izman, A. Shafaghat, A. Keyvanfar, and M.Z. Abd Majid, *J. Exp. Nanosci.* 11, 816 (2016).

10. M. Vallet-Regi and J.M. González-Calbet, *Prog. Solid State Chem.* 32, 1 (2004).
11. E. Mohseni, E. Zalnezhad, and A.R. Bushroa, *Int. J. Adhes. Adhes.* 48, 238 (2014).
12. M. Bahrami, M.H. Fathi, and M. Ahmadian, *Mater. Sci. Eng., C* 48, 572 (2015).
13. G. Lewis, *J. Mater. Sci. Mater. Med.* 24, 2293 (2013).
14. H. Kheimehsari, S. Izman, and M.R. Shirdar, *J. Mater. Eng. Perform.* 24, 2294 (2015).
15. M. Wei, A.J. Ruys, M.V. Swain, B.K. Milthorpe, and C.C. Sorrell, *J. Mater. Sci. Mater. Med.* 16, 101 (2005).
16. Z. Zhang, M.F. Dunn, T.D. Xiao, A.P. Tomsia, and E. Saiz, *MRS Proc.* 703, 291 (2011).
17. H.W. Kim, H.E. Kim, V. Salih, and J.C. Knowles, *J. Biomed. Mater. Res., Part A* 74, 294 (2005).
18. C.E. Wen, W. Xu, W.Y. Hu, and P.D. Hodgson, *Acta Biomater.* 3, 403 (2007).
19. A.A. Sagari, J. Malm, M. Laitinen, P. Rahkila, M. Hongqiang, M. Putkonen, M. Karppinen, H.J. Whitlow, and T. Sajavaara, *Thin Solid Films* 531, 26 (2013).
20. R.A. Gittens, R. Olivares-Navarrete, A. Cheng, D.M. Anderson, T. McLachlan, I. Stephan, J. Geis-Gerstorfer, K.H. Sandhage, A.G. Fedorov, F. Rupp, and B.D. Boyan, *Acta Biomater.* 9, 6268 (2013).
21. X. Rausch-fan, Z. Qu, M. Wieland, M. Matejka, and A. Schedle, *Dent. Mater.* 24, 102 (2008).
22. G. Zhao, A.L. Raines, M. Wieland, Z. Schwartz, and B.D. Boyan, *Biomaterials* 28, 2821 (2007).
23. Z. Chen, X. Zhang, Y. Yang, K. Zhou, N. Wragg, Y. Liu, M. Lewis, and C. Liu, *Ceram. Int.* 43, 336 (2017).
24. M. Farrokhi-Rad, S.K. Loghmani, T. Shahrabi, and S. Khanmohammadi, *J. Eur. Ceram. Soc.* 34, 97 (2014).
25. I. Corni, M.P. Ryan, and A.R. Boccaccini, *J. Eur. Ceram. Soc.* 28, 1353 (2008).
26. H.R. Bakhsheshi-Rad, E. Hamzah, M. Daroonparvar, S.N. Saud, and M.R. Abdul-Kadir, *Vacuum* 110, 127 (2014).
27. S. Shadanbaz and G.J. Dias, *Acta Biomater.* 8, 20 (2012).
28. M.R. Shirdar, S. Izman, H. Kheimehsari, N. Ahmad, and A. Ma'aram, *Surf. Innov.* 5, 90 (2017).
29. T.S. Hin, *Engineering Materials for Biomedical Applications*, Vol. 1 (Singapore: World Scientific, 2004).
30. M. Assadian, H. Jafari, S.M. Ghaffari Shahri, M.H. Idris, and B. Gholampour, *Surf. Eng.* 30, 806 (2014).
31. S. Hiromoto and A. Yamamoto, *Electrochim. Acta* 54, 7085 (2009).
32. U.U. Türkan, O. Öztürk, and A.E. Eroglu, *Surf. Coat. Technol.* 200, 5020 (2006).
33. M.R. Shirdar, S. Izman, M.M. Taheri, A. Keyvanfar, M.Z.M. Yusop, and M.R.A. Kadir, *Vacuum* 122, 82 (2015).
34. R. Junker, A. Dimakis, M. Thoneick, and J.A. Jansen, *Clin. Oral Implant Res.* 20, 185 (2009).
35. F. Schwarz, D. Ferrari, M. Herten, I. Mihatovic, M. Wieland, M. Sager, and J. Becker, *J. Periodontol.* 78, 217 (2007).
36. F. Rupp, R.A. Gittens, L. Scheideler, A. Marmur, B.D. Boyan, Z. Schwartz, and J. Geis-Gerstorfer, *Acta Biomater.* 10, 2894 (2014).